

UMSNet: An Universal Multi-sensor Network for Human Activity Recognition

Jialiang Wang

Haotian Wei

Yi Wang

Shu Yang

Chi Lin

Abstract

Human activity recognition (HAR) based on multimodal sensors has become a rapidly growing branch of biometric recognition and artificial intelligence. However, how to fully mine multimodal time series data and effectively learn accurate behavioral features has always been a hot topic in this field. Practical applications also require a well-generalized framework that can quickly process a variety of raw sensor data and learn better feature representations. This paper proposes a universal multi-sensor network (UMSNet) for human activity recognition. In particular, we propose a new lightweight sensor residual block (called LSR block), which improves the performance by reducing the number of activation function and normalization layers, and adding inverted bottleneck structure and grouping convolution. Then, the Transformer is used to extract the relationship of series features to realize the classification and recognition of human activities. Our framework has a clear structure and can be directly applied to various types of multi-modal Time Series Classification (TSC) tasks after simple specialization. Extensive experiments show that the proposed UMSNet outperforms other state-of-the-art methods on two popular multi-sensor human activity recognition datasets (i.e. HHAR dataset and MHEALTH dataset).

1. Introduction

Nowadays, people tend to utilize artificial intelligence (AI) to make their lives safe, health and smart. Human activity recognition (HAR) is an important basis for many practical applications, such as medical care [25], emotional response based on heart rate [11, 13], human activity monitoring [12], and health tracking [4]. HAR based on image data has been widely studied, but it has inevitable disadvantages: the limitation of usage scenarios, the issue of infringing personal privacy, and high requirements on the performance and storage of the image capture equipments. HAR based on time series data from wearable sensors can overcome the above problems. Many sensors have been integrated into mobile devices, such as mobile phones and watches, which can collect user data anytime and anywhere.

In addition, most of the data collected by sensors are physical quantities such as acceleration and angular velocity, which have little infringement on personal privacy.

Human activity recognition (HAR) based on multimodal wearable sensors is a challenging multivariate time series classification problem (TSC)[35]. Although many deep-learning based works have been done to solve multimodal feature extraction and fusion, spatial-temporal feature extraction, and classification problems involved in HAR, they still have limitation in real-world scenarios [35, 9, 10]. What is needed for practical applications is to build a framework with good generalizability that can quickly process raw sensor data and learn better feature representations.

To address the above issues, we propose a universal deep learning framework (UMSNet) for multi-modal time series classification. The core of the UMSNet is the integration of the residual network[24] and the Transformer[34]. The residual network is used to encode local and global multimodal features for sensors. The Transformer is used to learn spatial-temporal features. Particularly, to improve the performance of the residual network, we design a new and efficient lightweight sensor residual (LSR) block. LSR block reduces the number of activation function and normalization layers and uses an inverted bottleneck structure and grouping convolution. The entire framework can be easily customized with the Residual Net part and the Transformer part for a variety of identification tasks.

Specifically, the main contributions of this paper are as follows:

- **Framework contribution:** A universal multi-sensor learning (UMSNet) framework is proposed. The UMSNet is composed of the residual network and the Transformer, which can be applied to various multimodal time series classification (TSC) tasks.
- **Network contribution:** An efficient and lightweight sensor residual (LSR) block is proposed to fuse multimodal features. LSR block improves the performance by reducing the number of activation layers and normalization layers, and adding inverted bottleneck structure and grouping convolution. Use layerScale and stochastic depth as training strategies.

- Empirical contribution: The UMSNet achieves new state-of-the-art performance on two benchmark datasets(i.e., HHAR dataset and MHEALTH dataset).

2. Related Works

In this section, we briefly review the residual network, Transformer-based network, multi-modal network, human activity recognition, and related literatures. For more details, please refer to surveys[35, 10, 9].

2.1. Residual Network

With the raising and wide applications of deep-learning technology, classification models based on convolutional neural networks (CNNs) and their variants (e.g., fully convolutional neural networks (FCNs)[24]) have become the mainstream. VGGNet [28] improves the performance by increasing the number and depth of network layers on top of previous convolutional neural network (CNN) architectures. ResNet [15] builds on VGGNet by explicitly fitting a residual map implemented by a feed-forward neural network combined with shortcut connections. Then increase the network depth to obtain improved results. A remarkable aspect of another well-known network, GoogleLeNet [30], is that its architecture greatly improves the utilization of computing resources. In a well-designed network, the computational overhead remains the same as the model depth and width increase. SENet [18], the winner of the ILSVRC 2017 classification category, recalibrates the channel-wise feature responses without relying on new spatial dimensions. EfficientNet [31], a multidimensional hybrid model scaling method, greatly improves the training speed of the network. Regnet [27], like hand-designed networks, aims at interpretability, which can describe some general design principles for simple networks and generalize them in various settings. ConvNeXt [23] studies the architectural differences between ConvNets and Transformers, and identify confounding variables when comparing network performance. However, the design of residual network is not refined enough for the fusion of multimode data, and there are many parts that can be optimized.

2.2. Transformer-based Networks

The Transformer [34] has achieved great success in the field of artificial intelligence. Improvements to Transformer are also emerging. Bert [7] emphasizes that the traditional one-way language model or the method of shallowly splicing two one-way language models for pre-training is no longer used as before, but the new masked language model (MLM) is used for pre-training, so that deep bidirectional linguistic representations can be generated. Iz Beltagy et al. [2] propose a sparse attention mechanism that uses a combination of local self-attention and global self-attention (or sparse attention for short), and optimize it with CUDA

to maximize the model Capable of accommodating tens of thousands of texts in length while still achieving better results. Google proposed the Vision Transformer (ViT) [8], which can directly use Transformers to classify images without the need for convolutional networks. The ViT model achieves results comparable to current state-of-the-art convolutional networks, but requires significantly less computational resources for its training. MSRA propose a new visual Transformer called Swin Transformer [22], which can be used as a general backbone for computer vision, bringing the challenge of adapting Transformer from language to vision. However, using the Transformer alone, it is difficult to adapt to sensor data in a variety of data formats and requires a very large training set to achieve good results[14].

2.3. Multi-modal Network

QA Zhen et al. [26] propose to encode the time series of sensor data into images (i.e., encode a time series into a two-channel image) and use these transformed images to preserve the features required for human activity recognition. The Temporal Fusion Transformer (TFT) [21] proposes interpretable deep learning for time series forecasting. A novel attention-based architecture that combines high-performance multi-level forecasting with an interpretable understanding of temporal dynamics. Google proposed XMC-GAN [37], a cross-modal contrastive learning framework to train GAN models for text-to-image synthesis, for research addressing the problem of generated cross-modal contrastive loss. ALIGN [20] (A Large-scale Image and Noisy-Text Embedding) model, designed to address the problem that current vision and visual language SOTA models rely heavily on specific training datasets that require expert knowledge and extensive labels.

2.4. Human Activity Recognition

Deepsense [36] proposes a deep learning framework that runs on end devices, which can locally acquire sensor data that needs to be processed and apply deep learning models, such as convolutional neural networks, to these data without uploading to the cloud or gated recurrent neural networks. Bianchi V et al. [3] combine wearable devices with deep learning technology to propose a new human motion recognition system, the system uses convolutional neural networks to classify data on 9 different behaviors of users in a home environment and achieve a good classification effect. To characterize the relevance of the data in space, T-2DCNN and M-2DCNN convolutional network model [6] encoded the three-axis data of the inertial sensor into a data picture format, and then extracted the spatial correlation between the sensors and the temporal synchronization correlation characteristics of the three-axis data through convolution operation. Tufek N et al. [33] developed a human mo-

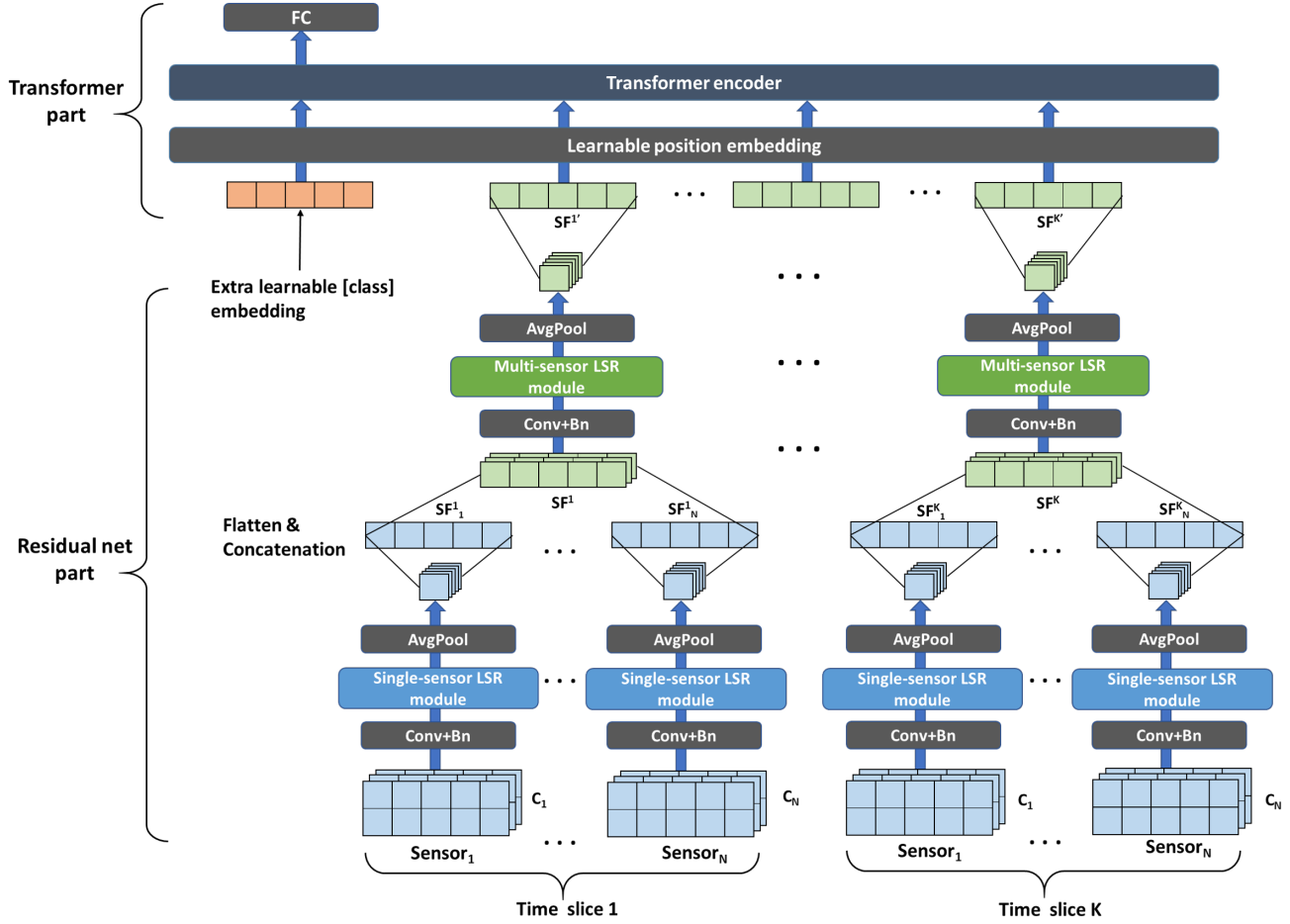


Figure 1. The structure of UMSNet. It is mainly composed of a Residual net part and a Transformer part. Lightweight sensor residual (LSR) module is the core of the Residual net part. The LSR Module consists of LSR blocks. Given a time series, the UMSNet processes it from bottom to top in three stages: single-sensor feature extraction, multi-sensor feature fusion and extraction, and multi-sensor sequence feature extraction and classification.

tion recognition system with using accelerometers and gyroscopes. The system utilizes a modified LSTM network to develop a behavioral classification system based on multi-type sensor data.

3. Methodology

3.1. Overview

In this section, we present the details of the proposed UMSNet. The network structure of UMSNet is shown in Figure 1. Given a time series X , the UMSNet processes it from bottom to top in three stages.

Stage 1: Single-sensor feature extraction. The proposed Lightweight sensor residual (LSR) module is used to carry out convolution operation to extract features, forming a unified sensor feature (SF_i^1) for the sensor i .

Stage 2: Multi-sensor feature fusion and feature extrac-

tion; In this stage, the features from N sensors are flattened and concatenated, and be taken as channels of a feature map of all sensors, named SF^K in each time slice K .

Stage 3: Multi-sensor sequence feature classification. The global information of N channels is merged into the $SF^{K'}$ and be input to the Transformer to get the classification results.

3.2. Lightweight Sensor Residual (LSR) Block

In order to improve the efficiency of multi-modal feature extraction of time series, we design a lightweight sensor residual block, called LSR block, by modifying the original residual network block structure. The LSR block is the core of the Single-sensor LSR module and the Multi-sensor LSR module in the UMSNet. The specific improvements are as follows:

- We first reduce the number of activation functions and

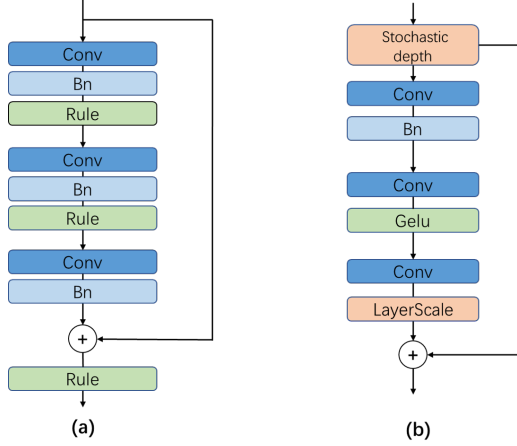


Figure 2. Illustration of the proposed Lightweight Sensor Residual (LSR) Block and the Resnet residual block[15]. (a): A Resnet residual block structure. (b): A LSR block structure.

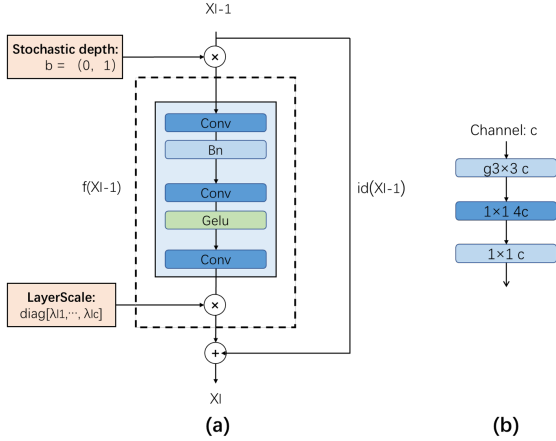


Figure 3. Details and an example of the LSR block. (a): Details of LayerScale and Stochastic depth in the LSR block. (b): An example of a channel change after convolution, where c is channel number, $[g3 \times 3]$ represents the grouping convolution layer with a $[3 \times 3]$ convolution kernel, and $[1 \times 1]$ represents the convolution layer with a $[1 \times 1]$ convolution kernel.

the number of normalization layers. As the ConvNeXt [23] network proves that too frequent nonlinear projections are actually detrimental to the information transfer of network features. So it is wise to use fewer activation functions and normalization in a residual block. The regular Resnet block uses three normalization layers and three activation functions, as shown in Figure 2(a). Here, in our new residual block, we only use one normalization layer and one activation function, as shown in Figure 2(b).

- Inspired by MobileNetV2 [17], we adopt the inverted

bottleneck structure in LSR block. Our LSR block in the form of small-large-small structure, as shown in Figure 3(b). In this way, information can be converted between feature spaces of different dimensions, avoiding information loss caused by dimension compression. Specifically, we expand the dimension of the input data to four times the original size in the second layer of convolution in the residual block. In the third layer of convolution, the dimensions are restored to the original size.

- We also replace the ordinary $[3 \times 3]$ convolutional layer with grouped convolution to make the network more lightweight. We use the maximum number of groups (the number of groups and the number of channels are the same), so that the number of parameters of the grouped convolutional layer is $\frac{1}{c}$ the public convolutional layer (c is the number of channels). This form of grouped convolution is similar to the self-attention mechanism, in which spatial information is mixed in a single channel because each convolution kernel processes a channel separately.

In addition, We use LayerScale [32] and Stochastic depth [19] as LSR block training strategies, as shown in Figure 3(a).

LayerScale: In the LSR block, different channels are multiplied by a parameter that can be learned to make features more refined and accurate. This process can be represented by the following equation:

$$x_{residual} = f(x_{l-1}) \times \text{diag}(\lambda_{l1}, \dots, \lambda_{lc}) \quad (1)$$

where f represents the residual part, $X_{residual}$ is the output of the residual link for this block, x_{l-1} is the output of the last LSR block, and $\lambda_{l1}, \dots, \lambda_{lc}$ are learnable parameters.

Stochastic depth: We use the stochastic depth to improve the generalization capability of the model. During training, a random variable b is added, satisfying the $(0 - 1)$ distribution, $x_{residual}$ is multiplied by b , and the residual part was randomly discarded. This process can be expressed by the following equation:

$$x_l = id(x_{l-1}) + bx_{residual} \quad (2)$$

where id represents the identity mapping, $X_{residual}$ is the output of the residual link for this LSR block, x_l is the output through this LSR block, x_{l-1} is the output of the last LSR block.

3.3. Transformer part

The Transformer part of UMSNet consists of Learnable Position embedding[8] and Transformer Encoder[34]. The Transformer part aims to extracting the sequence feature of sequence data.

The Transformer [34] is a model based on self-attention mechanism, which achieves higher accuracy and performance than conventional RNN. Here, we only use The Transformer Encoder to learn time series features. Before the Transformer Encoder, we add a learnable position embedding to each slice feature (SF') as position information. Meanwhile, inspired by Transformer-based Bert model [7], we insert a specific classification token ([class]) at the beginning of the time series. Both [class] and Position embedding are parameters of the network and can be learned and optimized automatically. The [class] token from the last Transformer layer is used to aggregate the entire series representation information. Finally, Fc (full connection layer) is used for classification.

Also, like Residual net part, you can customize the Transformer part with different parameters and depths depending on the task needs.

4. Experiments

4.1. Datasets

The following data sets are used for evaluating the performance of the proposed method.

HHAR[29] is a data set designed to serve as a benchmark for human activity recognition algorithms (classification, automatic data segmentation, sensor fusion, feature extraction, etc.) in real-world environments. Specifically, HHAR contains the readings from two motion sensors (i.e., the accelerometer and the gyroscope) in the smartphones and the smartwatches. This dataset contains six activities (i.e. cycling, sitting, walking, standing, walking upstairs, and walking downstairs) from nine users and six mobile devices (four smartphones and two smartwatches).

MHEALTH[1] is a mobile health data set based on multimodal wearable sensor data for the human activity recognition. Sensors are placed on the subjects' chest, right wrist and left ankle to measure movement of the body, using acceleration, angular velocity and magnetic field direction signals. In addition, the sensor placed on the chest provides two sets of lead to provide 2-lead Electrocardiograph measurements. Human activity in MHEALTH can be divided into seven categories, namely: standing, sitting and relaxing, lying down, walking, climbing stairs, cycling, and jogging.

4.2. Metrics

Since human activity recognition is a classification problem, each class can be regarded as an independent set of samples for the positive class, and the other classes for the negative class. Therefore, the classification performance is generally assessed by the Accuracy and Macro-F1 scores. The computational complexity of the network is evaluated by the Params, Multi-Adds and Time.

Accuracy [26] is the proportion of correctly identified examples in all samples and can be defined by

$$Accuracy = \frac{1}{n_{samples}} \sum_{i=1}^{n_{samples}} \iota(\hat{y}_i = y_i), \quad (3)$$

where \hat{y}_i is the predicted value of the i^{th} sample, y_i is the corresponding true value, and ι is the indicator function.

F1-score is an index used to measure the accuracy of multi-classification models in statistics, which is the harmonic mean of the Precision and the Recall. F1-score is defined by

$$F1_i = 2 \frac{Recall_i \times Precision_i}{Recall_i + Precision_i} \quad (4)$$

Macro-F1 [26] is suitable for multi-classification problems and is not affected by data imbalance. Given n class, $i \in (1, \dots, n)$, Macro-F1 is defined by

$$MacroF1 = \frac{\sum_{i=1}^n F1_i}{n} \quad (5)$$

Params refers to the number of parameters that can be learned and optimized in the network.

Multi-Adds indicates the number of arithmetic operations such as multiplication and addition on the network.

Time is needed to identify a sample of human activity (base on RTX3080).

4.3. Baseline Methods

We extensively evaluate the performance of the proposed UMSNet with several widely used architectures in HAR:

LSTM [16]: LSTM is a special RNN, which is mainly used to solve the problems of gradient disappearance and gradient explosion in the process of Long series training. In the experiments, we use the three-layer LSTM.

GRU [5]: GRU is an effective variant of the LSTM network, and its structure is simpler than that of LSTM network. In the experiments, we use the three-layer GRU.

Resnet [15]: Resnet use residual structure to solve the degradation problem, allows the network to deepen as much as possible. In the experiments, we use the Resnet50.

Efficientnet [31]: Efficientnet can improve the index and reduce the number and calculation of model parameters, by comprehensively optimizing network width, network depth and resolution. In the experiments, we use the Efficientnet-B1.

Regnet [27]: Regnet parameterizes the group of the network (e.g., Convolutional LSTMs or Convolutional GRUs), which are shown to be good at extracting Spatio-temporal information. In the experiments, we use the Regnet50.

Since the parameters of the LSR can be adjusted according to the needs of tasks and different sensor data formats

Depth	Single sensor LSR module	Multi-sensor LSR module	Transformer encoder
UMSNet-A	[2, 2, 2, 2]	[2, 2, 2, 2]	3
UMSNet-B	[2, 2, 6, 2]	[2, 2, 6, 2]	6
UMSNet-C	[2, 2, 18, 2]	[2, 2, 18, 2]	6

Table 1. The numbers in the table represent the quantity of the LSR blocks. For example, [2,2,2,2] represents a total of 8 LSR blocks, with a down sampled layer inserted between each two Residual blocks.

Method Comparison	$K = 6$		$K = 12$		$K = 24$	
	Accuracy	Macro-F1	Accuracy	Macro-F1	Accuracy	Macro-F1
GRU[5]	0.7858	0.7932	0.8378	0.8303	0.8474	0.8287
LSTM [16]	0.8093	0.8008	0.8398	0.8299	0.8564	0.8542
ResNet[27]	0.8815	0.8701	0.8936	0.8798	0.8808	0.8559
EfficientNet[31]	0.8991	0.9039	0.8964	0.8778	0.9052	0.8939
Regnet[27]	0.9079	0.9197	0.9079	0.9085	0.9166	0.9132
UMSNet-A(Ours)	0.9155	0.9093	0.9251	0.9312	0.9329	0.9342
UMSNet-B(Ours)	0.9171	0.9181	0.9304	0.9327	0.9358	0.9382
UMSNet-C(Ours)	0.9187	0.9211	0.9289	0.9304	0.9397	0.9402

Table 2. Performance of different methods on HHAR dataset. K is the slice number of a time series data.

and residual networks of different depths can be built, we design three kinds of the UMSNet with different structures in terms of the depths of the network for experiments as shown in Table 1, to demonstrate the flexibility of our network.

Method	Params	Multi-Adds	Time(ms)
GRU[5]	17712	17280	7.122
LSTM [16]	23616	23040	10.023
ResNet [27]	25.557M	4.089G	93.053
Efficientnet[31]	7.794M	569.682M	87.959
Regnet[27]	54.278M	15.940G	172.442
UMSNet-A	2.905M	72.863M	33.864
UMSNet-B	4.887M	76.564M	58.182
UMSNet-C	6.092M	82.944M	79.015

Table 3. Comparison of network parameter, computational cost, and the speed of processing a time series of 6 seconds on HHAR dataset.

4.4. Implementation details

Theoretically, the time length of each slice can be unequal in our UMSNet, which can be tuned according to the practical requirements. For a fair comparison, the time length of each slice is set to be equal for all methods. We divide the sequence data of two datasets into three time lengths of 1.5 seconds, 3 seconds, and 6 seconds, and we take 0.25s as a slice time length, so a time series X has three different sample numbers $K = 6, 12, 24$.

We used Gelu as the activation function to be consistent with Transformer. The down sampled layer between dif-

ferent residual blocks is composed of Bn plus a $[2 \times 2]$ convolution with $stride = 2$.

4.5. Experimental results on HHAR dataset

The HHAR data set has two types of sensors, an acceleration sensor and a gyroscope (angular velocity sensor). The x , y , and z axes of each sensor are taken as the three channels of input data.

For all methods, the leave-one-user-out test method is used, that is, for the 9 users in the HHAR data set, 8 users are taken as the training set and another user is taken as the test set to test each user. Experimental results are presented in Table 2, Figure 4 and Table 3.

Experimental results show that our methods are superior to other SOTA methods in terms of accuracy and macro-F1 over three-length settings of times series. It can be seen from the accuracy curves (in Figure 4) of the three time slice lengths that the recognition rate of all algorithms increases with the increase of the sample number of a time series. In particular, recognition rate of the three structures of our UMSNet increases stably, indicating the stability of our network designs. Other methods, such as Resnet and Efficientnet, are all irregular and unstable.

In addition, the network computation cost of UMSNet is far less than the conventional residual network based classification network, i.e., ResNet[15] and Regnet[27], in Table 3. Although the network parameters and computation cost of the UMSNet are larger than that of the simple RNN networks, i.e., GRU[5] and LSTM[16], the accuracy of the UMSNet is far better than that of them. The UMSNets improves accuracy about 10% – 14% than on GRU[5] and LSTM[16] on average. All these results show the effec-

Method comparison	$K = 6$		$K = 12$		$K = 24$	
	Accuracy	Macro-F1	Accuracy	Macro-F1	Accuracy	Macro-F1
GRU[5]	0.878	0.876	0.9337	0.933	0.9187	0.9203
LSTM[16]	0.8455	0.8417	0.9145	0.9142	0.9346	0.9341
ResNet[27]	0.9707	0.9706	0.9701	0.9701	0.9714	0.9713
Efficientnet[31]	0.9783	0.9782	0.9714	0.9713	0.9736	0.9735
Regnet[27]	0.9785	0.9785	0.9813	0.9814	0.9836	0.9836
UMSNet-A(Ours)	0.9797	0.9798	0.983	0.9829	0.9852	0.9851
UMSNet-B(Ours)	0.9802	0.9802	0.9842	0.9842	0.9857	0.9856
UMSNet-C(Ours)	0.9804	0.9804	0.9844	0.9844	0.9872	0.9872

Table 4. Performance of different methods on MHEALTH dataset. K is the slice number of a time series data.

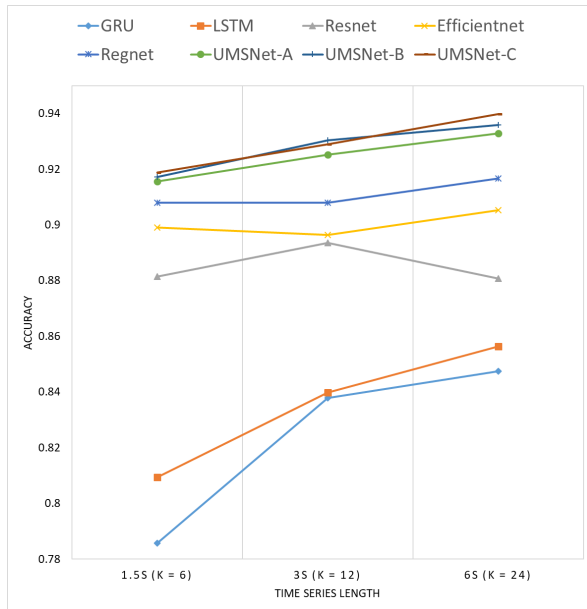


Figure 4. Accuracy of different methods of three time series length setting on HHAR dataset.

tiveness of UMSNet.

4.6. MHEALTH

MHEALTH dataset has four kinds of sensors, i.e., acceleration sensor, angular velocity sensor, magnetometer, and electrocardiograph sensor. Acceleration sensors, angular velocity sensors, and magnetometers have x, y, and z axes, which we use as 3 channels. The electrocardiograph sensor has 2 leads, which we use as 2 channels. It is worth noting that even if the format of Sensor data is different, we can also customize the UMSNet by using the proposed sensor LRS module. The evaluation methods for MHEALTH dataset are similar to that of the HHAR dataset. Experimental results are presented in Table 4, Figure 5, and Table 5.

It can be observed from results that UMSNet-C achieves excellent performance in the MHEALTH dataset. Because

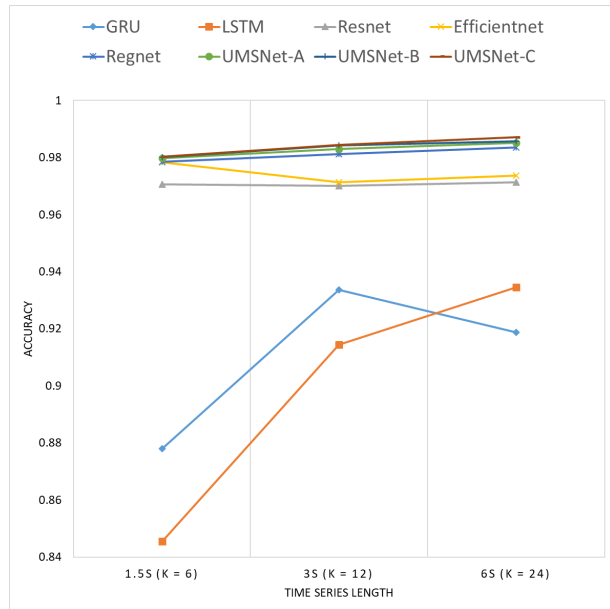


Figure 5. Accuracy of different methods of three time series length setting on MHEALTH dataset.

Method	Params	Multi-Adds	Time(ms)
GRU[5]	28704	28560	2.958
LSTM[16]	38272	38080	4.082
ResNet[15]	25.557M	4.089G	90.996
Efficientnet[31]	7.794M	569.682M	75.981
Regnet[27]	54.278M	15.940G	168.266
UMSNet-A	5.555M	36.056M	49.565
UMSNet-B	8.340M	39.550M	68.284
UMSNet-C	11.955M	45.307M	119.418

Table 5. Comparison of network parameter, computational cost, and the speed of processing a time series of 6 seconds on MHEALTH dataset.

MHEALTH dataset has more kinds of sensors than HHAR dataset, all methods improve the accuracy of recognition to

a certain extent. However, it can be seen from Figure 5 that our methods still maintains robustness. Considering the network performance and recognition rate comprehensively in Table 4 and Table 5, our overall performance is better than other methods.

Experimental results on these two datasets show that the proposed UMSNet has good generalization and performance for multiple sensor time series.

5. Conclusion

In this paper, we propose the UMSNet framework for human activity recognition. The UMSNet integrates the fusion residual network and Transformer structure to automatically extract local, global, and time series relationships from multimodal sensors to effectively perform classification tasks. We evaluated the UMSNet using two representative human activity datasets (i.e. HHAR, MHEALTH), in which the UMSNet outperforms other state-of-the-art networks. UMSNet is smaller in network complexity than other networks, requiring very few computing resources to train the network. We have also designed three UMSNet architectures to provide experience for broad application and further adaptation and customization of the framework. In the future, we intend to extend this work to other multimodal tasks, as well as to use other (larger) datasets for evaluation.

References

- [1] O. Banos, R. Garcia, J. A. Holgado-Terriza, M. Damas, H. Pomares, I. Rojas, A. Saez, and C. Villalonga. mhealth-droid: a novel framework for agile development of mobile health applications. In *International workshop on ambient assisted living*, pages 91–98. Springer, 2014.
- [2] I. Beltagy, M. E. Peters, and A. Cohan. Longformer: The long-document transformer. *arXiv preprint arXiv:2004.05150*, 2020.
- [3] V. Bianchi, M. Bassoli, G. Lombardo, P. Fornacciari, M. Mordonini, and I. De Munari. Iot wearable sensor and deep learning: An integrated approach for personalized human activity recognition in a smart home environment. *IEEE Internet of Things Journal*, 6(5):8553–8562, 2019.
- [4] A. Bulling, U. Blanke, and B. Schiele. A tutorial on human activity recognition using body-worn inertial sensors. *ACM Computing Surveys (CSUR)*, 46(3):1–33, 2014.
- [5] J. Chung, C. Gulcehre, K. Cho, and Y. Bengio. Empirical evaluation of gated recurrent neural networks on sequence modeling. *arXiv preprint arXiv:1412.3555*, 2014.
- [6] S. Deng, B. Wang, C. Yang, and G. Wang. Convolutional neural networks for human activity recognition using multi-location wearable sensors. *J. Softw.*, 30(3):718–737, 2019.
- [7] J. Devlin, M.-W. Chang, K. Lee, and K. Toutanova. Bert: Pre-training of deep bidirectional transformers for language understanding. *arXiv preprint arXiv:1810.04805*, 2018.
- [8] A. Dosovitskiy, L. Beyer, A. Kolesnikov, D. Weissenborn, X. Zhai, T. Unterthiner, M. Dehghani, M. Minderer, G. Heigold, S. Gelly, et al. An image is worth 16x16 words: Transformers for image recognition at scale. *arXiv preprint arXiv:2010.11929*, 2020.
- [9] S. A. Ebrahim, J. Poshtan, S. M. Jamali, and N. A. Ebrahim. Quantitative and qualitative analysis of time-series classification using deep learning. *IEEE Access*, 8:90202–90215, 2020.
- [10] H. I. Fawaz. Deep learning for time series classification. *arXiv preprint arXiv:2010.00567*, 2020.
- [11] G. Fortino, S. Galzarano, R. Gravina, and W. Li. A framework for collaborative computing and multi-sensor data fusion in body sensor networks. *Information Fusion*, 22:50–70, 2015.
- [12] H. Ghasemzadeh, P. Panuccio, S. Trovato, G. Fortino, and R. Jafari. Power-aware activity monitoring using distributed wearable sensors. *IEEE Transactions on Human-Machine Systems*, 44(4):537–544, 2014.
- [13] R. Gravina and G. Fortino. Automatic methods for the detection of accelerative cardiac defense response. *IEEE Transactions on Affective Computing*, 7(3):286–298, 2016.
- [14] K. Han, A. Xiao, E. Wu, J. Guo, C. Xu, and Y. Wang. Transformer in transformer. *Advances in Neural Information Processing Systems*, 34, 2021.
- [15] K. He, X. Zhang, S. Ren, and J. Sun. Deep residual learning for image recognition. In *Proceedings of the IEEE conference on computer vision and pattern recognition*, pages 770–778, 2016.
- [16] S. Hochreiter and J. Schmidhuber. Long short-term memory. *Neural computation*, 9(8):1735–1780, 1997.
- [17] A. Howard, A. Zhmoginov, L.-C. Chen, M. Sandler, and M. Zhu. Inverted residuals and linear bottlenecks: Mobile networks for classification, detection and segmentation. 2018.
- [18] J. Hu, L. Shen, and G. Sun. Squeeze-and-excitation networks. In *Proceedings of the IEEE conference on computer vision and pattern recognition*, pages 7132–7141, 2018.
- [19] G. Huang, Y. Sun, Z. Liu, D. Sedra, and K. Q. Weinberger. Deep networks with stochastic depth. In *European conference on computer vision*, pages 646–661. Springer, 2016.
- [20] C. Jia, Y. Yang, Y. Xia, Y.-T. Chen, Z. Parekh, H. Pham, Q. Le, Y.-H. Sung, Z. Li, and T. Duerig. Scaling up visual and vision-language representation learning with noisy text supervision. In *International Conference on Machine Learning*, pages 4904–4916. PMLR, 2021.
- [21] B. Lim, S. Ö. Arik, N. Loeff, and T. Pfister. Temporal fusion transformers for interpretable multi-horizon time series forecasting. *International Journal of Forecasting*, 37(4):1748–1764, 2021.
- [22] Z. Liu, Y. Lin, Y. Cao, H. Hu, Y. Wei, Z. Zhang, S. Lin, and B. Guo. Swin transformer: Hierarchical vision transformer using shifted windows. In *Proceedings of the IEEE/CVF International Conference on Computer Vision*, pages 10012–10022, 2021.
- [23] Z. Liu, H. Mao, C.-Y. Wu, C. Feichtenhofer, T. Darrell, and S. Xie. A convnet for the 2020s. *arXiv preprint arXiv:2201.03545*, 2022.

- [24] J. Long, E. Shelhamer, and T. Darrell. Fully convolutional networks for semantic segmentation. In *Proc. IEEE Conf. Comput. Vis. Pattern Recognit.*, pages 3431–3440, Boston, MA, USA, 2015.
- [25] S. Mazilu, U. Blanke, M. Hardegger, G. Tröster, E. Gazit, and J. M. Hausdorff. Gaitassist: a daily-life support and training system for parkinson’s disease patients with freezing of gait. In *Proceedings of the SIGCHI conference on Human Factors in Computing Systems*, pages 2531–2540, 2014.
- [26] Z. Qin, Y. Zhang, S. Meng, Z. Qin, and K.-K. R. Choo. Imaging and fusing time series for wearable sensor-based human activity recognition. *Information Fusion*, 53:80–87, 2020.
- [27] I. Radosavovic, R. P. Kosaraju, R. Girshick, K. He, and P. Dollár. Designing network design spaces. In *Proceedings of the IEEE/CVF Conference on Computer Vision and Pattern Recognition*, pages 10428–10436, 2020.
- [28] K. Simonyan and A. Zisserman. Very deep convolutional networks for large-scale image recognition. *arXiv preprint arXiv:1409.1556*, 2014.
- [29] A. Stisen, H. Blunck, S. Bhattacharya, T. S. Prentow, M. B. Kjærgaard, A. Dey, T. Sonne, and M. M. Jensen. Smart devices are different: Assessing and mitigating mobile sensing heterogeneities for activity recognition. In *Proceedings of the 13th ACM conference on embedded networked sensor systems*, pages 127–140, 2015.
- [30] C. Szegedy, V. Vanhoucke, S. Ioffe, J. Shlens, and Z. Wojna. Rethinking the inception architecture for computer vision. In *Proceedings of the IEEE conference on computer vision and pattern recognition*, pages 2818–2826, 2016.
- [31] M. Tan and Q. Le. Efficientnet: Rethinking model scaling for convolutional neural networks. In *International conference on machine learning*, pages 6105–6114. PMLR, 2019.
- [32] H. Touvron, M. Cord, A. Sablayrolles, G. Synnaeve, and H. Jégou. Going deeper with image transformers. In *Proceedings of the IEEE/CVF International Conference on Computer Vision*, pages 32–42, 2021.
- [33] N. Tufek, M. Yalcin, M. Altintas, F. Kalaoglu, Y. Li, and S. K. Bahadir. Human action recognition using deep learning methods on limited sensory data. *IEEE Sensors Journal*, 20(6):3101–3112, 2019.
- [34] A. Vaswani, N. Shazeer, N. Parmar, J. Uszkoreit, L. Jones, A. N. Gomez, Ł. Kaiser, and I. Polosukhin. Attention is all you need. *Advances in neural information processing systems*, 30, 2017.
- [35] J. Wang, Y. Chen, S. Hao, X. Peng, and L. Hu. Deep learning for sensor-based activity recognition: A survey. *Pattern Recognition Letters*, 119:3–11, 2019.
- [36] S. Yao, S. Hu, Y. Zhao, A. Zhang, and T. Abdelzaher. Deepsense: A unified deep learning framework for time-series mobile sensing data processing. In *Proceedings of the 26th international conference on world wide web*, pages 351–360, 2017.
- [37] H. Zhang, J. Y. Koh, J. Baldrige, H. Lee, and Y. Yang. Cross-modal contrastive learning for text-to-image generation. In *Proceedings of the IEEE/CVF Conference on Computer Vision and Pattern Recognition*, pages 833–842, 2021.